

High throughput laser micro machining on a rotating cylinder with ultra short pulses at highest precision

B. Jaeggi*^a, B. Neuenschwander^a, T. Meier^b, M. Zimmermann^b, G. Hennig^c

^aBern University of Applied Sciences, Institute for Applied Laser, Photonics and Surface Technologies, Pestalozzistrasse 20, CH-3400 Burgdorf, Switzerland

^bBern University of Applied Sciences, Institute for Mechatronic Systems, Pestalozzistrasse 20, CH-3400 Burgdorf, Switzerland

^cDaetwyler Graphics AG, Flugplatz, CH-3368 Bleienbach, Switzerland

ABSTRACT

For surface and 3D structuring ultra-short pulsed laser systems are used in combination with mechanical axes, whereas the mechanical axes can include electrical motor as well as beam deflecting systems like a galvo scanner. The motion of the axes is synchronized with the clock of the laser pulses, which is usually in the range of 100 kHz and above, by a modification of the electronic axes control. This work shows the scalability of the ablation process up to MHz-regime in relation to surface quality and ablation efficiency. Furthermore the transfer of the machining strategy from a synchronized galvo scanner to a rotating cylinder setup is shown. **Keywords:** Ultra short pulsed laser system, galvo scanner, rotating cylinder, synchronization, scalability of the ablation process, MHz-ablation

1. INTRODUCTION

A standard process for surface structuring applications is the filling of a given outline with a parallel hatching. 3D structures are built up with successive 2D slices (figure 1a) into the third dimension. The series of slices have an adapted outline, which is filled with lines. By ablating slice by slice the 3D structure occurs (figure 1b). This process is called 2.5D processing.

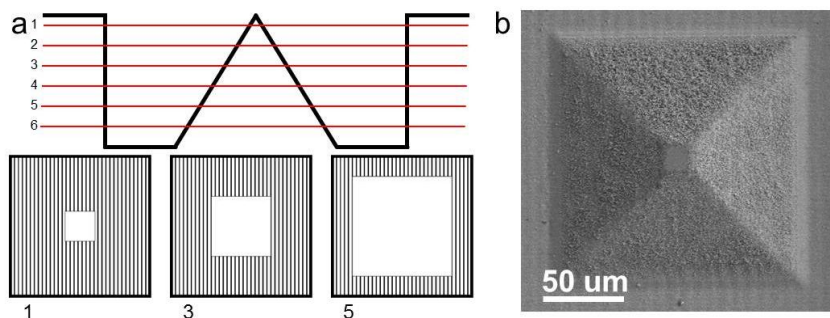


Figure 1: 2.5D process a) successive 2D slices; b) SEM image of a machined 3D-structure in Copper

The lines of the hatch pattern are generated with mechanical axes including electrical motors like linear motor and / or a beam deflecting systems, whereupon the laser pulse train is switched on and off via an external modulator which is gated by a signal from the axes control and / or beam deflecting system software. Figure 2 shows the different situations that can appear at the border of a structure. If the pulse train is switched on with the start of the axes acceleration the distance from pulse to pulse (pitch) increases until the axes has reached its final speed (figure 2a). Such lines show deep marks at the start and ending points of the single lines but the effective position of these points are well defined.

*beat.jaeggi@bfh.ch; phone +41 (0)34 426 41 93; fax +41 (0)34 423 15 13;

To avoid this, a so called sky-writing option can be used i.e. the axes already have the correct velocity at the beginning of the marking. With this option a displacement of the start position of plus/minus the distance between two consecutive pulses has to be accepted (figure 2b). For highest precision it is necessary to synchronize the axes motion onto the output pulse train of the laser system or vice versa (figure 2c).

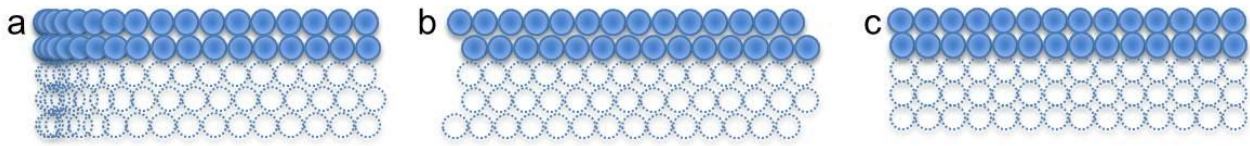


Figure 2: Start positions of the different strategies: a) without sky-writing; b) with sky-writing; c) synchronized system

The today available industrially suited ultra-short pulsed systems are turnkey systems, set up in a master oscillator power amplifier (MOPA) arrangement with a passively mode locked seed laser. Therefore normally it is not possible to control the phase of the pulse train and the motion of the mechanical axes has to be synchronized with the laser pulse train. This problems are already shown in literature^{1,2}. In a first task the best machining strategy with respect to minimum surface roughness and structure dimension was investigated by using the synchronized galvo scanner. With repetition rates in the range of 100 kHz to 300 kHz and 532 nm wavelength we have shown the advantages and possibilities of the synchronized machining^{1,2}. On a polished copper target a minimum surface roughness of 90 nm *Ra*-value was achieved, machined with a pitch of half of the spot radius w_0 . The minimum structure dimension which could be achieved was in the range of one spot radius. 3D structures were obtained by generating the corresponding bitmaps for each slice and working with the normal 2.5D process and random distributed starting values for each slice as described above.

To increase the competitiveness of micromachining with ultra-short laser pulses the process time i. e. the throughput is one of the key factors. For fast micromachining a fast deflection system is needed. With the galvo scanner we use a feed rate of 8 m/s. This speed needs a repetition rate in the MHz-regime in order to have an overlapping of the consecutive pulses. We show in this work the scalability of the process by linear increasing the repetition rate up to 1 MHz, the average power and the marking speed. Additionally by using a rotating sample like a rotating cylinder even higher processing speeds can be achieved. The transfer of the machining strategy from the galvo scanner to the rotation setup and the using of 2 MHz repetition rate are shown, as well. In industrial applications such cylinders are used as embossing-cylinders.

2. EXPERIMENTAL SETUP

All experiments were performed with a DUETTO system (Time Bandwidth Products) generating 10 ps pulses at 1064 nm and 532 nm wavelength with repetition rates from 50 kHz to 8.2 MHz. The laser light was always circular polarized by using a $\lambda/4$ -waveplate. The laser pulse train was monitored with an internal photodiode and the exact repetition rate and phase of the pulse train were electronically deduced. These were fed to an own developed control software synchronizing the motion of the galvo-mirrors and the axes of the rotating cylinder. With the synchronized set-up the machining strategy was changed from vector-scanning to a pixel representation where one pixel represents one "laser-shot" during the motion of the axes^{1,2}. Basic black and white bitmaps serve as input for the control software.

In a first experiment the machining strategy and the scalability of the process was tested on a flat sample using a synchronized galvo scanner (figure 3) for deflecting the laser beam. The machining of small flat samples gives the possibility to test different machining strategies and analyze them with different microscopes. To work at the point where the ablation process is most efficient a specific peak fluence has to be used. A detailed discussion on this subject will follow in the next section. By increasing the repetition rate, also the average power has to be increased. This is insofar possible as the limit of the laser system is reached concerning the average power. Until this limit is reached, the unique factor to increase the repetition rate again, is to reduce the spot radius by changing the focal optic. At the same average power the maximum achievable repetition rate is higher for a smaller spot radius. The used scanner system was an IntelliScan_{de}14 with a 100 mm telecentric objective for 532 nm and a 160 mm f-theta objective for 1064 nm. The spot radius w_0 was 5.7 μm for 532 nm and 16.3 μm for 1064 nm, respectively, and the beam quality M^2 was smaller than 1.3, both measured with a slit scanning beam profiler. The sample material was copper Cu-DHP (in US: C12 200) whose surface was polished with a 3 μm diamond suspension. Due to the used objectives, the maximum used repetition rate amounts 1 MHz.

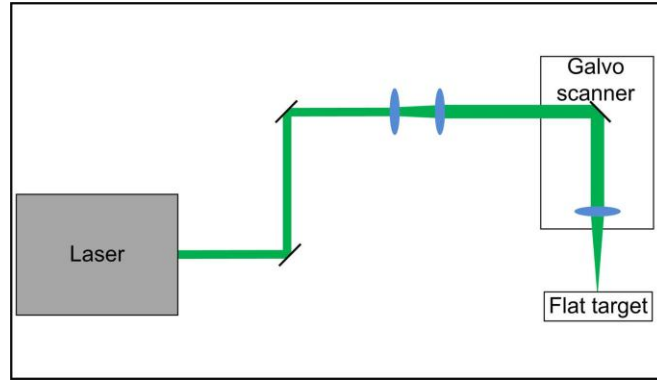


Figure 3: Scanner Setup for machining the flat samples

In order to go to higher repetition rates a second experiment structuring a cylinder surface was performed using one rotation and one linear axis, which both were synchronized on the laser pulse train (figure 4). The diameter of the cylinder was 150 mm and the wavelength of the processing laser was of 532 nm. The laser beam was focused with a lens with a focal length of $f = 75$ mm resulting in a spot radius of w_0 of $4 \mu\text{m}$ and a beam quality M^2 smaller than 1.3. With this spot radius repetition rates up to 2MHz could be tested on the cylindrical set up. The machined cylinder is a steel cylinder with an electro-plated copper coating.

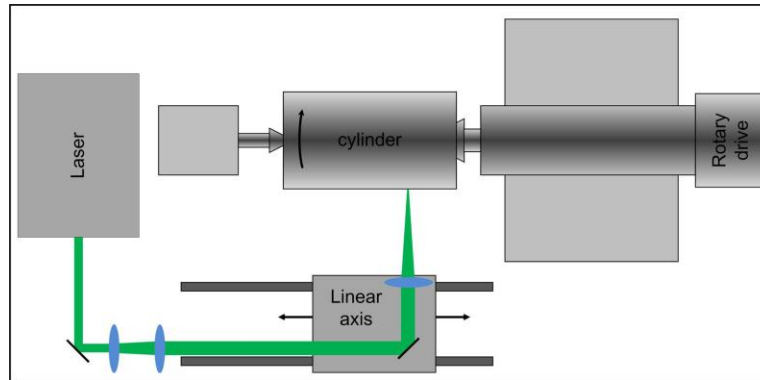


Figure 4: Setup for machining the rotating cylinder

3. THEORETICAL BACKGROUND

As a consequence of the two-temperature-model which is discussed in the literature³⁻¹⁰, the logarithmic ablation law between the peak laser fluence in the beam center ϕ_0 of the laser pulse and the ablation depth z_{abl} is given by:

$$z_{abl} = \delta \cdot \ln\left(\frac{\phi_0}{\phi_{th}}\right) \quad (1)$$

The ablation depth z_{abl} depends on the two material parameters energy penetration depth δ and threshold fluence ϕ_{th} . The threshold fluence ϕ_{th} describes the minimum energy which is needed to ablate material. The energy penetration depth δ is the ability of the energy to penetrate into the material. These material parameters have an important role in precision laser micro machining. For a Gaussian beam the maximum material removal rate $\Delta V/(\Delta t * W)_{max}$ reads¹¹⁻¹³:

$$\left(\frac{\Delta V/\Delta t}{P_{av}}\right)_{max} = \frac{2}{e^2} \cdot \frac{\delta}{\phi_{th}} \quad (2)$$

The ablation process shows this maximum possible efficiency at a certain peak fluence:

$$\phi_0 = e^2 \cdot \phi_{th} \quad (3)$$

The optimum pulse energy E_p can be written as a function of the beam radius w_0 and the threshold fluence ϕ_{th} :

$$E_p = \frac{\pi \cdot w_0^2}{2} \cdot \phi_{th} \cdot e^2 \quad (4)$$

The pulse energy was chosen for all experiments to work close to this optimum point. The threshold fluence for 512 pulses applied and a wavelength of 532 nm is 0.11 J/cm² and 0.31 J/cm² for 1064 nm respectively. The energy penetration depth is 6.67 nm for 532 nm and 31.7 nm for 1064 nm. With the used spot radii this leads in case of the synchronized scanner to pulse energies of 0.41 μJ for 532 nm and 9.2 μJ for 1064 nm. For the rotating cylinder the used pulse energy was 0.2 μJ due to the smaller spot radius compared to the galvo scanner. Therefore the maximum useable repetition rate, where the pulse energy is sufficient for ablating, is higher.

4. RESULTS AND DISCUSSION

4.1 Synchronized galvo scanner

Figure 5 shows a sequence of machined Tux, the icon of Linux¹⁴ in copper with 1064 nm using the 2.5D processing method with 100 different layers. The repetition rate was increased from 200 kHz (figure 5a) to 1 MHz (figure 5d). To work at the optimum point, for 1 MHz repetition rate an average power of 9.25 W is needed. Due to the limit of the laser system the average power was 8.6 W instead of the 9.25 W. If heat accumulation occurs, the surface quality will decrease with increasing repetition rates. Comparing the SEM images in figure 6, no decrease of the surface quality is observed for the increasing repetition rates. The small melting worms on the surface are for all repetition rates on the same scale, so the heating accumulation has no influence. Similar results concerning the influence of heat accumulation have been seen at the wavelength of 532 nm and repetition rates up to 1 MHz as shown in figure 7.

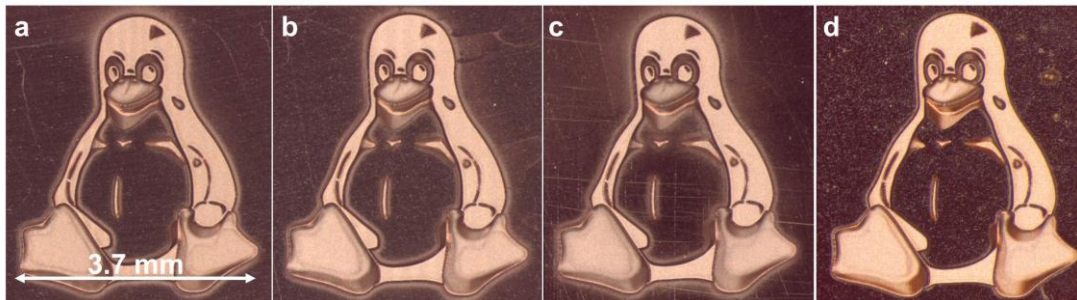


Figure 5: Sequence of Tux machined with a wavelength of 1064 nm and marking speeds from 1.6 m/s to 8 m/s a) 200 kHz, 1.8 W; b) 300 kHz, 2.8 W; c) 500 kHz, 4.6 W; d) 1 MHz, 8.6 W

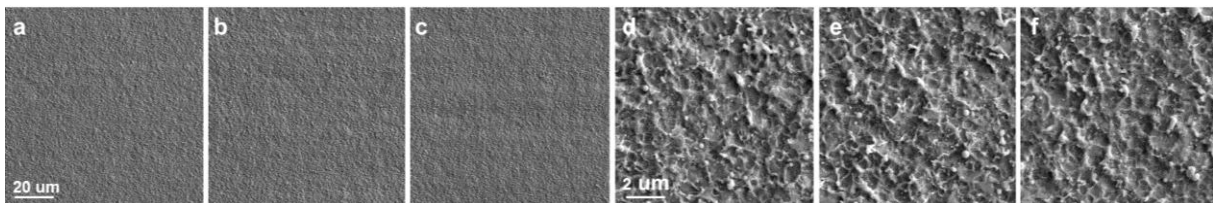


Figure 6: SEM images of the surface quality of Tux a) 200kHz; b) 500kHz; c) 1MHz; d) Detail view of a; e) Detail view of b; f) detail view of c

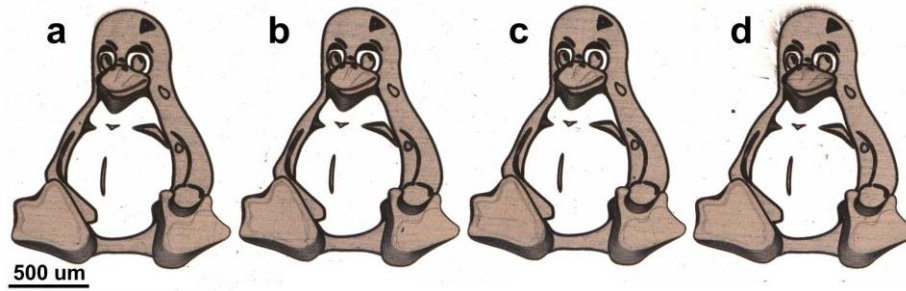


Figure 7: Sequence of Tux machined with 532 nm wavelength and markings speeds from 0.9 m/s up to 3m/s
 a) 300 kHz, 120mW; b) 500kHz, 204mW, c) 700kHz, 280mW; d) 1 MHz, 408mW

Another way to analyze the scalability of the process is the comparison of the depths of the structures. If particle shielding^{15,16} take place, a significant reduce of the structure depth with increased repetition rate should be observed. A comparison of the achieved structure depths shows no significant differences between low and high repetition rates. The depth are 25.2 μm for 100 kHz and 28.92 μm for 1 MHz in case of 1064 nm wavelength and 16.75 μm for 300 kHz and 15.69 μm for 1 MHz in the case of 532 nm, respectively. With the used machining strategy, the limit of the repetition rate, where the heat accumulation and/or the particle shielding have a strong influence, was not reached. Therefore the scalability of the ablation process by changing the repetition rate up to 1 MHz is proofed. The high accuracy concerning the position during full motion of the scanner is shown in figure 8. During one layer one pulse per cavity appears and it is clearly seen in the detail view (figure 8c,d), that all 30 pulses strikes on the same point even at a speed of 8 m/s.

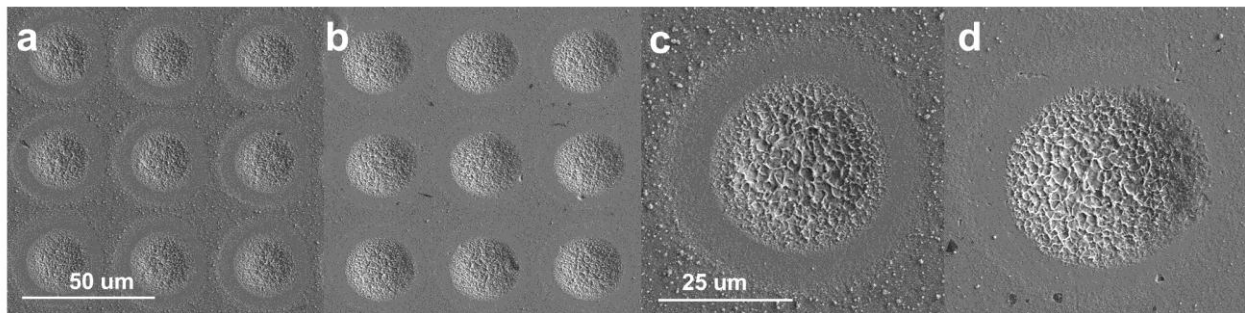


Figure 8: SEM images of cavities machined on the fly; a) 200kHz, 2W, 1.6m/s, 30 layers; b) 1MHz, 8.6W, 8m/s, 30 layers; c) detail view of a; d) detail view of b

4.2 Rotating cylinder

The discovered strategy is transferred from a flat sample to a rotating cylinder where the higher speeds offered the possibility to work with repetition rates higher than 1 MHz. With this setup it is possible to strike the same position on the cylinder during the motion with an accuracy of about 1 μm up to a repetition rate of 2 MHz as shown in figure 9a. The rotation speed of the cylinder was 8.5 rps which correlate to a relative slow surface speed of 4 m/s due to the small spot size. Red marked cavities in figure 8a were shot twice and the other only once with an average power of 0.6 W at a repetition rate of 2 MHz. The next step is to machine a 3D structure as shown in the figures 9b and 9c. In order to use the same machining strategy it is necessary to have the random distribution of the starting points^{1,2}. Therefore during the backwards motion of the linear stage to the starting point of the new layer, the rotary motion is delayed for this random starting value. The inner part of the two squares in figure 9b consists of 60 layers whereas the outer part only consists of 30 layers. The checkerboard pattern in figure 9c consists of 30 layers. The black and white images are the same for each slice, only the starting points are different. Other examples are shown in figure 10. To machine the rose (figure 10a) one black and white bitmap is used ablating it 30 times. The next step is to machine a greyscale image, which is divided into 100 different black and white images, like the Tux, shown in figure 10b. Figure 10c shows a coherent checkerboard pattern, which is marked around the cylinder without any optical effects at the intersection marked in the image.

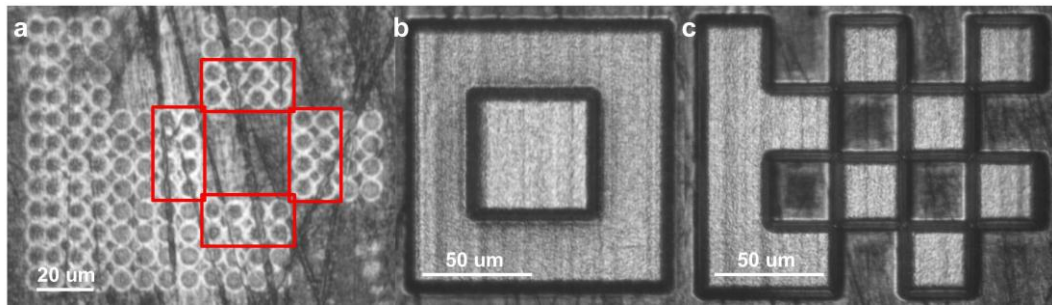


Figure 9: Images on the cylinder a) Cavities, 2 MHz, 0.6W; b) Squares, 2 MHz, 0.6 W; c) Checkerboard pattern, 2 MHz, 0.6 W

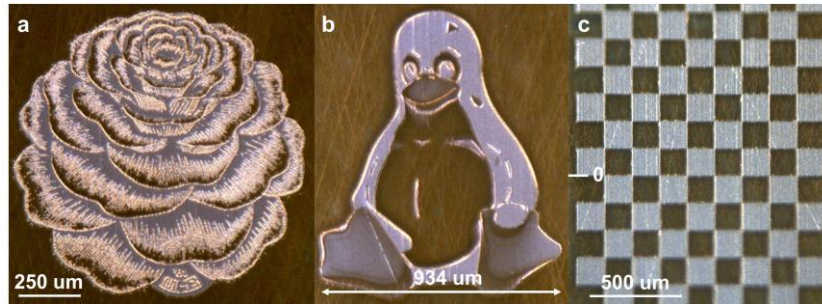


Figure 10: a) Rose¹⁷, 2 MHz, 0.6 W, 30 layers; b) Tux¹⁴, 2 MHz, 0.6 W, 100 layers; c) Coherent checkerboard pattern, 2 MHz, 0.6 W, 20 layers, intersection at the zero-mark

5. SUMMARY AND OUTLOOK

In a first step with the galvo scanner setup, the scalability of the machining process was demonstrated by linearly increasing the repetition rate, the average power and the marking speed up to 8 m/s in the case of 1064 nm and 3 m/s for 532 nm, respectively. No difference of the surface quality is observed between the different average powers. Also the ablation efficiency is nearly constant. In case of the used machining strategy, the heat accumulation and the particle shielding do not take place for repetition rates up to 1 MHz. Additionally we have shown that it is possible to machine a rotating cylinder with synchronized rotating and linear axes. The machining strategy can be transferred from the synchronized galvo scanner to the rotating cylinder. For both setups it is possible to strike the same point twice during full motion of the mirrors or the axes. For the cylinder setup in future the next step is to change the wavelength from 532 nm to 1064 nm and to enlarge the spot radius. Due to this increase of the spot radius the mark speed increases as well. These two factors lead to an average power in the range of 10 W and a repetition rate between 2 and 3 MHz. With the industrially suited laser system this repetition rates are the limit where the AOM can pick single pulses. To operate with single shots and higher repetition rates i.e. some MHz, the optical setup of the AOM has to be changed. But then the minimum repetition rate of the laser system is in the MHz range due to the high peak fluences at repetition rates of some kHz in the AOM and its damage threshold. The introduction of an additional fast deflector as a third synchronized axis¹⁸, offers new opportunities to decrease the process time and will allow to use even higher average powers of several 10 W. These high powers are achievable by using the same laser system with an additional amplifier.

ACKNOWLEDGMENT

The authors wish to thank Josef Zuercher for his help with the SEM images. This work is supported in parts by the Bern University of Applied Sciences Engineering and Information Technology and the Swiss Commission for Technology and Innovation CTI.

REFERENCES

- [1] Jaeggi B., Neuenschwander B., Hunziker U., Meier T., Zimmermann M., Hennig G. et al., "Ultra-high-precision surface structuring by synchronizing a galvo scanner with an ultra-short-pulsed laser system in MOPA arrangement," Proc. SPIE 8243, (2012)
- [2] Jaeggi B., Neuenschwander B., Hunziker U., Zuercher J., Meier T., Zimmermann M. et al., "High precision and high throughput surface structuring by synchronizing mechanical axes with an ultra short pulsed laser system in MOPA arrangement," paper M1207, ICALEO (2012)
- [3] Nolte S., "Mikromaterialbearbeitung mit ultrakurzen Laserpulsen," Dissertation, Duvillier Verlag, Göttingen,
- [4] Nolte S., Momma C., Jacobs H., Tünnermann A., Chichkov B.N., Wellegehausen B. et al., "Ablation of metals by ultrashort laser pulses," J. Opt. Soc. Am. B / Vol 14, No. 10 / October (1997)
- [5] Körner C., "Theoretische Untersuchungen zur Wechselwirkung von ultrakurzen Laserpulsen mit Metallen," Dissertation der technischen Fakultät der Universität Erlangen-Nürnberg, (1997)
- [6] Chichkov B.N., Momma C., Nolte S., von Alvensleben F., Tünnermann A., "Femtosecond, picosecond and nanosecond laser ablation of solids," Appl. Phys. A 63, 109-115 (1996)
- [7] Momma C., Nolte S., Chichkov B.N., von Alvensleben F., Tünnermann A., "Precise laser ablation with ultrashort pulses", Appl. Phys. Sci. 109/110, 15-19 (1997)
- [8] C. Momma, B.N. Chichkov, S. Nolte, F. von Alvensleben, A. Tünnermann, H. Welling et al., "Short-pulse laser ablation of solid targets," Opt. Commun. 129, 134-142 (1996)
- [9] Christensen B.H., Vestentoft K. and Balling P., "Short-pulse ablation rates and the two-temperature model," Appl. Surf. Science 253, 6347-6352 (2007)
- [10] Anisimov S.I. and Rethfeld B., "On the theory of ultrashort laser pulse interaction with a metal," Proc. SPIE 3093, 192-203 (1997)
- [11] Neuenschwander B., Bucher G., Hennig G., Nussbaum C., Joss B., Muralt M., Zehnder S. et al., "Processing of dielectric materials and metals with ps laserpulses," ICALEO 2010, Paper M101 (2010)
- [12] Raciukaitis G., Brikas M., Gecys P., Voisiat B., Gedvilas M., "Use of High Repetition Rate and High Power Lasers in Microfabrication: How to keep Efficiency High?," JLMN Journal of Laser Micro/Nanoengineering; Vol. 4 (3), p186-191 (2009)
- [13] Neuenschwander B., Bucher G., Nussbaum C., Joss B., Muralt M., Hunziker U. et al., "Processing of dielectric materials and metals with ps-laserpulses: results, strategies limitations and needs," Proceedings of SPIE vol. 7584, (2010)
- [14] <http://en.wikipedia.org/wiki/File:Tux.svg>
- [15] Ancona A., Röser F., Rademaker K., Limpert J., Nolte S. and Tünnermann A., "High speed laser drilling of metals using a high repetition rate, high average power ultrafast fiber CPA system," Opt. Express, Vol. 16, 8958-8968 (2008)
- [16] König J., Nolte S., Tünnermann A., "Plasma evolution during metal ablation with ultrashort laser pulses," Opt. Express, Vol. 13, 10597-10607 (2005)
- [17] http://www.zazzle.ch/rosen_lithographie_fotoskulptur-153582013095294502
- [18] Bruening S., Hennig G., Eifel S., Gillner A., "Ultrafast Scan techniques for 3D-um Structuring of Metal Surfaces with high repetitive ps laser pulses," Physics Procedia 12, 105-115 (2011)